

Thermal consequences of lithosphere extension over continental margins: the initial stretching phase

F. Alvarez, J. Virieux and X. Le Pichon *Laboratoire de Géodynamique, LA 215, Université P. et M. Curie, Tour 15, Et, 4 Place Jussieu, 75230 Paris Cedex 05, France*

Received 1983 December 8; in original form 1983 July 25

Summary. We compute the thermal evolution of a lithosphere submitted to stretching during a finite duration of time in order to discuss the initial stretching phase of future continental margins. The numerical method developed can handle 2-D laterally variable stretching as well as sedimentation. It is shown that lateral conduction is more important than vertical conduction over most continental margins during their formation by stretching. A simple way to evaluate the relative importance of lateral and vertical conduction effects at the axis of the zone of rifting just prior to oceanization is proposed. A simple way to evaluate the amplitude of the thermal uplift on the edges of the zone of rifting at the end of the stretching phase is also presented. For small width zones of rifting (< 70–100 km) lateral cooling becomes so large as to prevent large-scale melting and, presumably, prevent the transition to oceanization. The effect of high-sedimentation rates (100–500 m Myr⁻¹) is to increase the surface temperature of the lithosphere and consequently significantly decrease the surface heat flow.

Introduction

The homogeneous extension of the lithosphere under isostatic equilibrium has been proposed by McKenzie (1978) as a mechanism of subsidence. His initial model assumed instantaneous extension followed by vertical cooling of the lithosphere. These assumptions lead to very simple formulations of the initial subsidence produced by instantaneous stretching and of the total subsidence after an infinite time (McKenzie 1978; Le Pichon, Angelier & Sibuet 1982). Although the model may seem overly simplistic, it appears to describe reasonably well the formation of many continental basins and margins (e.g. Sclater & Christie 1980; Royden, Sclater & Von Herzen 1980; Royden & Keen 1980; Le Pichon & Sibuet 1981). It is now generally agreed that extension is indeed a widespread cause of formation of basins and continental margins.

It is consequently necessary to explore more carefully the limitations introduced by the assumptions initially made by McKenzie (1978). In this paper, we concentrate on the

rifting phase. This is for example the situation prevailing at the present time in the Gulf of Suez (Angelier & Coletta 1983) and in the North Aegean trough (Le Pichon, Lyberis & Alvarez 1984). In both places, active stretching affects a zone about 100 km wide since 10–20 Myr ago. Subsidence has been amplified by the continuous infill of terrigenous sediments which, locally, exceeds a thickness of 3–5 km. We ask the following questions: What is the effect of the finite duration of rifting? What is the effect of the rapid lateral variations in stretching as the width of the rifting zone is equivalent to the thickness of the lithosphere? What is the effect of the rapid infilling of sediments? We deliberately ignore the possible mechanical complexities and assume local isostatic equilibrium and homogeneous thinning over the whole thickness of the lithosphere. Le Pichon *et al.* (1984) have shown that the first assumption is verified in the North Aegean trough where the elastic lithosphere appears to have a negligible effective thickness and that the second assumption is not incompatible with available data. We thus evaluate the thermal effects for continental margins during their formation phase of the simplest possible mechanical model of laterally variable homogeneous lithosphere stretching under variable sedimentation.

The effect of a finite duration of stretching in the absence of lateral conduction (the one-dimensional, 1-D, case) has been evaluated analytically by Jarvis & McKenzie (1980). However, more complex models require the use of numerical methods. This has been done by De Bremaecker (1984) with a finite element method to investigate the additional effect of sedimentation in the 1-D case. His results indicate that heat flow is significantly modified by the presence of sedimentation at rates above 0.1 km Myr^{-1} . We show in this paper that lateral conduction introduces significant changes in the evolution of the rifting phase. Actually, we conclude that it may prevent the formation of an accreting plate boundary if the rifting zone is too narrow. On the other hand, we show that although the perturbation due to sedimentation is large for heat flow, it is generally negligible for tectonic subsidence.

We first present the physical model based on the heat transfer equation, the particle velocity field description and an optional sedimentary perturbation which accounts for the thermal blanketing sedimentary effects. The numerical discretization scheme and the evaluation of the velocity field are presented more fully in Appendices A and B respectively. Our numerical solutions are validated, in the 1-D case, by comparison with the analytical solutions of Jarvis & McKenzie (1980) and Carslaw & Jaeger (1959). We then evaluate the effects of lateral variations in stretching on surface heat flow and subsidence. Finally, we discuss the effects of high sedimentation rates during the rifting phase.

Problem formulation

Consider the lithosphere as a collection of particles moving along trajectories defined by velocity field $\mathbf{v}(x, z, t)$ in the plane (Oxz) where axis Oz is pointing downwards (in direct frame). The governing equation can be written in a fixed reference frame (Oxz) under its general form

$$\rho C_p \left(\frac{\partial T}{\partial t} + \mathbf{v} \cdot \text{grad } T \right) = k \Delta T + A \quad (1)$$

with a mass conservation condition that is reduced to

$$\text{div } \mathbf{v} = 0 \quad (2)$$

because ρ , the density of the medium, is assumed to be explicitly independent of time. C_p is the heat capacity, k the conductivity and A the heat generation term. Dividing

equation (1) by ρC_p , we introduce the diffusivity $\kappa = k/\rho C_p$. Table 1 presents values for parameters used in this study in the SI system.

The numerical method used is an immediate extension of the 'splitting-up' method (ADI) of Peaceman & Racheford (1955) and Douglas (1955) which gives an absolutely stable, second-order (in space and time) scheme when only the conductive terms are considered (see Marchuk 1975 for example). The extension of this method to the solution of the equation with convective terms gives a second-order (in space and time) scheme which is no longer absolutely stable because the velocities of the particles change with time. In spite of this mathematical restriction, we have not found any unstable behaviour for the velocity interval commonly assumed in lithosphere extension. Therefore, there was no need to use more complex numerical formulations that are shown to be absolutely stable under conditions of smoothness (Marchuk 1975). The numerical discretization is explicated in Appendix A.

The basic assumption we use to describe the velocity field is that the horizontal strain rate $\dot{\epsilon}_x$ is independent of depth as well as time for a given moving column of particles. Equation (2) implies further

$$\dot{\epsilon}_x = -\dot{\epsilon}_z = -1/z \, dz/dt = g \quad (3)$$

where g is constant through depth and time for a given column of particles. Thus, within the mobile reference frame fixed to a column of particles, the finite relative extension can be obtained by integration

$$\beta = \exp(g\Delta t). \quad (4)$$

Note that β and g are respectively the finite and instantaneous extension factors of McKenzie (1978) and Jarvis & McKenzie (1980).

Table 1. Parameters for thermal computation and main symbols used.

Lithosphere

Thermal conductivity	$k_L = 3.1395$	$\text{W m}^{-1} \text{K}^{-1}$
Coefficient of thermal expansion	$\alpha = 3.28 \times 10^{-5}$	
Thermal capacity	$c_L = 1.172 \times 10^3$	$\text{J kg}^{-1} \text{K}^{-1}$
Thermal diffusivity	$\kappa_L = 8.04 \times 10^{-7}$	$\text{m}^2 \text{s}^{-1}$
Thickness of crust	$h_c = 3 \times 10^4$	m
Thickness of lithosphere	$h_L = 1.25 \times 10^5$	m
Density of crust at 0°C	$\rho_c = 2.78 \times 10^3$	kg m^{-3}
Density of mantle at 0°C	$\rho_m = 3.35 \times 10^3$	kg m^{-3}
Temperature of asthenosphere	1333°C	
Grid mesh	5×10^3	m
Time increment	$5 \times 10^5 \text{ yr}$	
Finite extension factor	β with $\gamma = 1 - 1/\beta$	
Half-width of rifting zone at the end of rifting	$L, \text{ km}$	
Subsidence under water	$S, \text{ m}$	
Height of uplift on the edges of the rifting zone at the end of rifting	$B, \text{ m}$	

Sediments

Thermal conductivity	$k_s = 2.10 - 0.97 \exp(-z/1210)$	$\text{W m}^{-1} \text{K}^{-1}$
Volumetric heat capacity	$\rho_s c_s = 2.09 \times 10^6 + 2.09 \times 10^6 \exp(-z/1210)$	$\text{J m}^{-3} \text{K}^{-1}$
Density	$\rho_s = (2.52 - 1.39) \times 10^3 \exp(-z/1210)$ $= 2.52 \times 10^3 - 1.39 \times 10^3 \exp(-z/1210)$	kg m^{-3}

Sea-water

Density	$1.03 \times 10^3 \text{ kg m}^{-3}$
Temperature	0°C

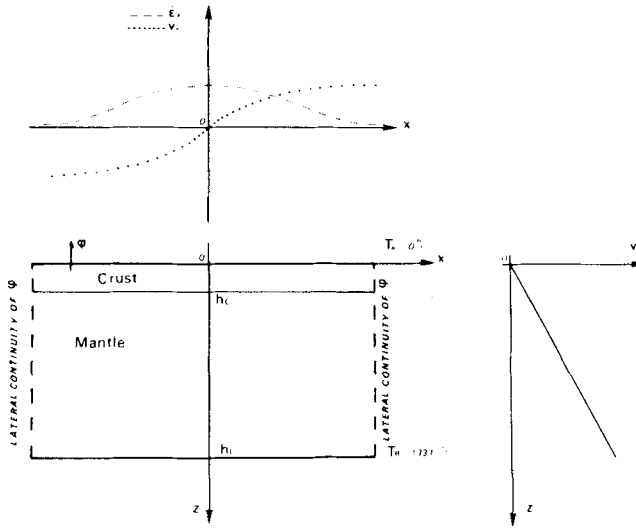


Figure 1. Physical model geometry. Before extension, the h_L thick lithosphere has a h_C thick crust. At the top of the figure, the horizontal velocity, and associated instantaneous coefficients, are presented along the profile. On the right, vertical velocity is shown with respect to the depth.

As g does not change with time for a given column of particles, the distribution $g(l)$ is independent of time in a deformable reference frame (l) fixed to the particles where

$$g(l) = 1/l \, dl/dt. \tag{5}$$

The problem, then, is to resolve (5) to obtain $g(l)$ and to go from the $g(l)$ to the $g(x, t)$ at a given time t . In practice, we compute the deformation of the grid by numerical interpolation, starting from the an initial stage and using spline functions (see Appendix B). *Note that this allows us either to impose a distribution $g(x, 0)$ in the initial undeformed state or to give the distribution with respect to the final extended state $g(x, T)$ based for example on the present distribution of finite extension factor $\beta(x)$.* In the later case, the program will do the necessary contraction of the basin to find the initial distribution $g(x, 0)$.

Then, knowing $g(x, t)$, we obtain the velocity field v at each instant by using the equations

$$v_x(x, t) = \int_{x_0}^x g(u, t) \, du \tag{6}$$

$$v_z(x, z, t) = g(x, t) \cdot z$$

with $v_x(x_0, t) = 0$ at the origin of the frame (generally chosen at the axis of the basin to minimize numerical integration errors) and with $v_z(x, 0, t) = 0$ on the free surface (see Fig. 1). When stretching ceases, v is identified to $\mathbf{0}$ everywhere.

The thermal boundary conditions chosen are fixed temperatures at the top ($z = 0$) and bottom ($z = h_L$, where h_L is the thickness of the lithosphere). Continuity of heat flow is imposed through the vertical boundaries to avoid any heat accumulation on them. Any initial distribution of temperatures may be imposed. In this paper, we assume steady thermal state in the absence of convection. If the heat production is null, the temperature gradient is linear. In the case of heat production, we choose

$$A(z) = A_0 \exp(-Z/D) \tag{7}$$

within the crust and $A(Z)=0$ in the mantle. Then, knowing $T(z=0)$ and assuming continuity of heat flow and temperature, we solve

$$k \frac{\partial^2 T}{\partial Z^2} + A(Z) = 0. \tag{8}$$

This imposes a value of $T(h_L)$ which depends on $A(Z)$. For consistency, we have chosen $A(Z)$ such that $T(h_L) = T_a$ where h_L (thickness of lithosphere) and T_a (temperature of asthenosphere) are constants which do not change whatever the initial distribution of temperature (see Fig. 2).

The sedimentation perturbation method

We treat the thermal effect of the sediments as a perturbation by relaxing the temperature condition at the top surface of the lithosphere. This can be done if the sedimentary cover is considered to be a thin insulating layer in instantaneous thermal equilibrium with the heat flow at its base and the imposed surface temperature. Then, knowing the heat flow at its base, which is the heat flowing out of the lithosphere, we compute the temperature at the base of the sedimentary layer which becomes the new top surface temperature $T_x(0, t)$ for the lithosphere. We then make a second-order correction to obtain the heat flow at the surface of the sediments, taking into account the heat absorbed by the sediments because of their increasing thickness and increasing average temperature. At each time step, new average thermal parameters are computed for the sedimentary layer (see Appendix C). Note that the thin layer approximation implies that the sediment thickness h_s is small with respect to the length of penetration of the thermal perturbation caused by the sediments

$$h_s \ll \sqrt{2\kappa t} \tag{9}$$

where t is the total sedimentation time. Note that it also implies that heat is only flowing vertically through the sedimentary cover.

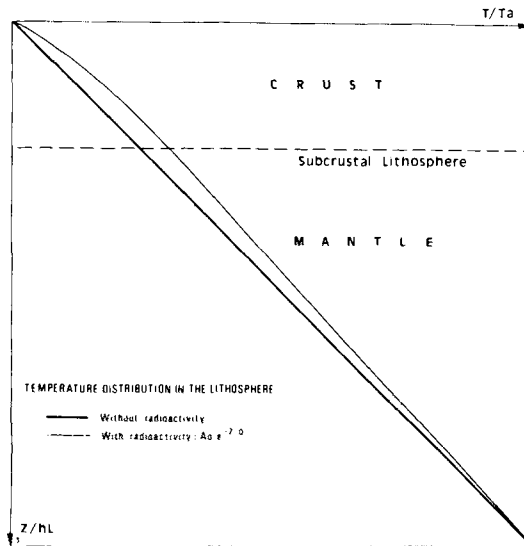


Figure 2. Initial lithospheric temperature distribution with or without radioactivity in the crust.

We treat the sedimentation in the same way as the velocity field, considering that it is fixed to the moving column of particles. Then, knowing the sedimentation history for each column of particles, we go from the mobile to the fixed frame by the interpolation described above. For the computations made in this paper, we have assumed a linear increase of sediments through time for each column of particles, independently of the extension rate. As discussed in Appendix C, the average density of the sedimentary layer is assumed to depend only on its thickness. Thus, a linear increase of the sedimentary cover with time requires a sedimentation rate which increases through time because the sedimentary cover is also stretched and because it is continuously compacted. This rather artificial hypothesis is adopted here for simplicity of computations although the sedimentation history could have been made as complex as we like.

Computations of thermal subsidence (or uplift)

We assume a lithosphere of no lateral rigidity floating on an asthenosphere which has its upper surface at a constant depth h_L . Thus the level $Z = h_L$ is an isobaric surface. If m_0 is the initial reference mass of the lithospheric column and m_t the mass of this column at time t , the subsidence under waters is

$$S = (m_t - m_0)/(\rho_a - \rho_w) \quad (10)$$

where ρ_a is the density of the asthenosphere and ρ_w the density of water. Above water, ρ_w is set equal to zero. Note that the thermal computations method used does not take into account the deformation of the grid due to thermal expansion and consequently does not conserve mass (Beaumont, Keen & Boutillier 1982). But this error does not affect the estimation of the subsidence with the hypothesis made here that the level of compensation is at a constant depth and consequently that the thickness of the lithosphere changes slightly with expansion. Note also that, if there is no stretching ($\beta = 1$), the only variation in topography of the upper surface of the lithosphere is due to thermal expansion. One has

$$S = \alpha h_L (\bar{T}_0 - \bar{T}_t) \cdot \rho_a / (\rho_a - \rho_w) \quad (11)$$

where \bar{T}_t is the average temperature of the lithosphere at time t and \bar{T}_0 is the initial average temperature of the lithosphere. S is negative (corresponding to uplift) when $\bar{T}_t > \bar{T}_0$.

The computation of topography in the presence of sediments is then obtained with

$$h_w = S - h_s(\rho_a - \bar{\rho}_s)/(\rho_a - \rho_w) \quad (12)$$

where h_w is the depth of water at the top of the sedimentary layer.

Unidimensional computations

We first tested our numerical method with the analytical solution proposed by Jarvis & McKenzie (1980) in the case of unidimensional uniform stretching of a lithosphere without sedimentation. The accuracy of our solution is excellent in all the tested cases, using stretching durations as long as 20 Myr and values of β as high as 3.25. Computations were extended to 300 Myr to test the return to thermal equilibrium.

We next tested the sedimentation perturbation method using the analytical solution proposed by Carslaw & Jaeger (1959, p. 388) for a homogeneous medium with an initial linear temperature gradient and a constant upward movement of the free surface. This

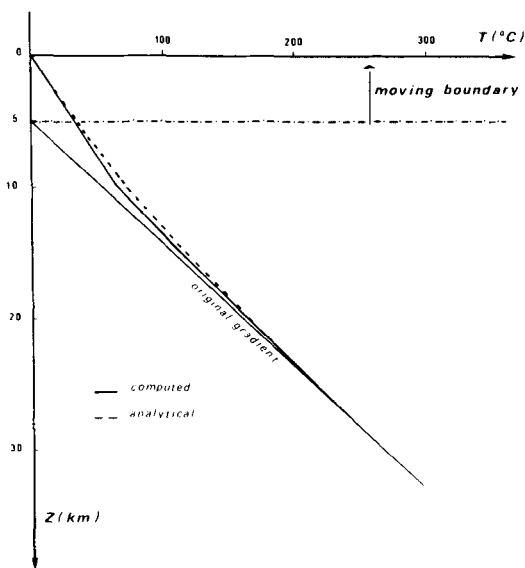


Figure 3. Sedimentary perturbation; comparison between the numerical solution and the analytical solution for an initial linear thermal gradient of $1.06 \times 10^{-2} \text{ }^\circ\text{C m}^{-1}$ and for a sedimentary rate of 500 m Myr^{-1} (without compaction).

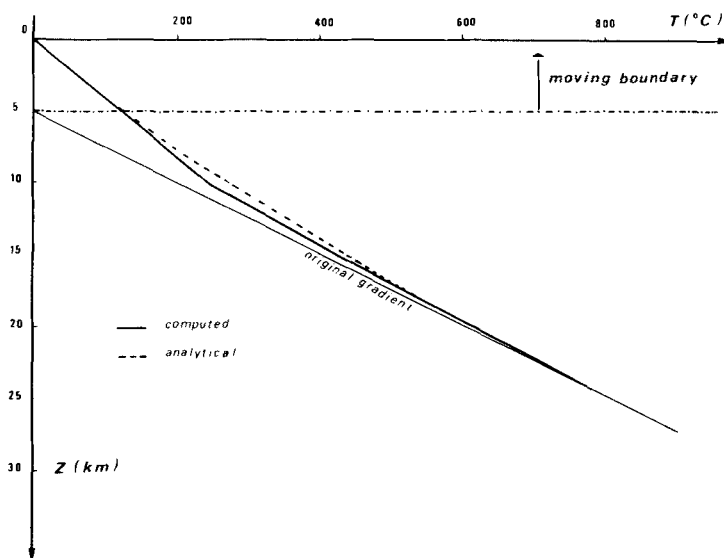


Figure 4. Sedimentary perturbation; comparison between the numerical solution and the analytical solution for an initial linear thermal gradient of $4.16 \times 10^{-2} \text{ }^\circ\text{C m}^{-1}$ and for a sedimentary rate of 500 m Myr^{-1} (without compaction).

simulates unidimensional constant rate sedimentation without compaction in the absence of extension ($\beta = 1$). We considered both a 'normal' equilibrium temperature (in the absence of radioactivity) of $1.06 \times 10^{-2} \text{ }^\circ\text{C m}^{-1}$ and a high (four times higher) gradient. The diffusivity was chosen equal to the adopted lithospheric diffusivity ($0.804 \times 10^{-6} \text{ m}^2 \text{ s}^{-1}$, see Table 1). This value is about 15 per cent too large for the equivalent diffusivity of a 5 km

thick sedimentary column (as discussed later) but the analytical solution does not allow for a changing diffusivity with depth. The spatial discretization step used is 5 km and the time is 0.5 Myr. In spite of the relatively coarse grid used, the accuracy of the method is still fairly good at sedimentation rates of 200 m Myr⁻¹ (better than 4 per cent). It deteriorates rapidly at rates higher than 500 m Myr⁻¹ (maximum error of 16 per cent).

Figs 3 and 4 show the temperature profiles after 10 Myr of sedimentation at 500 m Myr⁻¹ for both 'normal' and 'high' temperature gradients. It is seen that the problem is well related to the spatial discretization step, the maximum error occurring at the first node below the sedimentary interface. However, as 500 m Myr⁻¹ is a high sedimentation rate for basins produced by stretching and continental margins in general, this method can be used to obtain with reasonable accuracy estimates of the thermal effect of the sedimentation cover in most geological cases. Its advantages are, of course, simplicity and a small computing time.

Bidimensional computations without sedimentation

We now consider idealized extensional basins produced by a linear symmetrical distribution of $\beta(x)$ over a final width (after extension) of 100 and 300 km. The linear distribution is chosen because the thickness of crust, over many continental margins, varies approximately linearly with distance (Le Pichon & Sibuet 1981). The 100 km width corresponds to the smallest width described for a set of margins (the Corsican and Provençal margins which are 50 km wide each, Le Douaran, Burrus & Avedik 1984). The 300 km width corresponds approximately to the width of a double East American margin (150 km, e.g. Le Pichon & Sibuet 1981). Thus, the two cases described span the complete range of continental margins which have been described. We have also assumed that the crust thins to a minimum thickness of 5 km from an original thickness of 30 km, as on the Armorican margin for example (Le Pichon & Sibuet 1981), this stretching corresponds to a maximum β of 6. Finally, the duration of extension is chosen to be 10 Myr, which is small compared to the Armorican margin but is comparable to the time of stretching of the West Mediterranean margins (Le Douaran *et al.* 1984). Thermal relaxation is computed during another 10 Myr.

We assume no radioactivity and parameters as in Table 1. At the beginning, with thermal equilibrium, the lithosphere is in isostatic equilibrium with a 2.5 km water depth ridge crest. In the absence of oceanic crust, the asthenosphere would rise to 3.6 km instead of 2.5 km and thus instantaneous infinite stretching would produce a subsidence from sea-level to 3.6 km water depth. Le Pichon *et al.* (1982) have shown that the instantaneous stretching of a lithosphere originally at sea-level produces a subsidence S under water

$$S = 3600(1 - 1/\beta) = 3600\gamma \text{ in metres.} \quad (13)$$

Thus subsidence increases linearly with γ which is the proportion of lithosphere instantaneously removed by stretching (McKenzie 1978). Figs 5 and 6 show the evolution of the distribution of heat flow and of the subsidence (or uplift) with time. For comparison, the corresponding distribution at 10 Myr, assuming instantaneous stretching, using (13), is shown in Fig. 5.

Fig. 5 clearly shows that the effect of conduction is to increase the subsidence considerably and decrease the heat flow with respect to the instantaneous stretching solution of (13). In addition, as noted for example by Beaumont *et al.* (1982), an uplift appears on the edges of the zone of extension which reaches an absolute value equal to 12 per cent of the maximum subsidence. This uplift and corresponding increased heat flow in a zone of no extension is obviously the result of lateral conduction.

We consequently need to investigate more closely the role of lateral conduction with

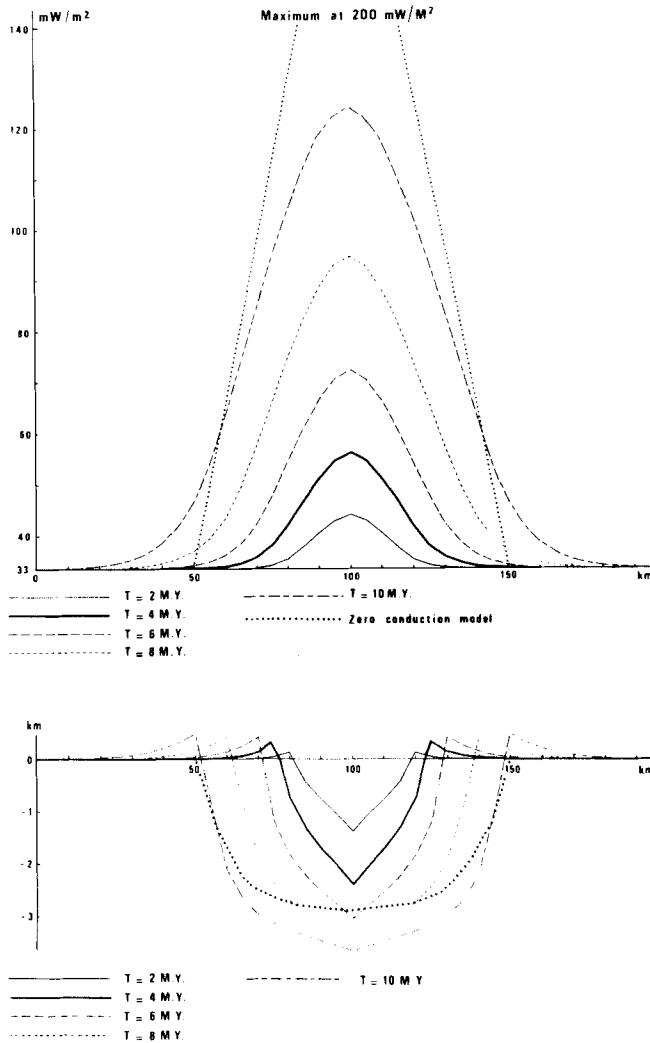


Figure 5. Thermal evolution of a hypothetical basin with a final width of 100 km. The extension factor distribution is symmetrical, with a maximum extension factor of 6 after 10 Myr. Thermal flux and subsidence are displayed during the extension phase, every 2 Myr. The instantaneous stretching solution is plotted for comparison.

respect to vertical conduction. To do that, we compare bidimensional computations with unidimensional ones and with instantaneous stretching solutions (using equation 13) in Figs 7–10. Subsidence and heat flow distributions for 10 and 30 Myr are shown for a basin with a final width of 100 km (Figs 7 and 8) and 300 km (Figs 9 and 10). In both cases, β reaches a maximum of 6 at the axis at the end of the extensional process. In both cases, if stretching were instantaneous, one would obtain an axial heat flow of 200 mW m^{-2} and an axial subsidence of 3 km (equation 13).

Call ϕ_1 and S_1 the surface heat flow and the subsidence without conduction, ϕ_2 and S_2 with only vertical conduction, ϕ_3 and S_3 with both vertical and lateral conduction. We consider the heat flow vertical conduction effect $E_V = \phi_1 - \phi_2$ and the heat flow lateral conduction effect $E_L = \phi_2 - \phi_3$. Similarly, we consider the subsidence vertical conduction

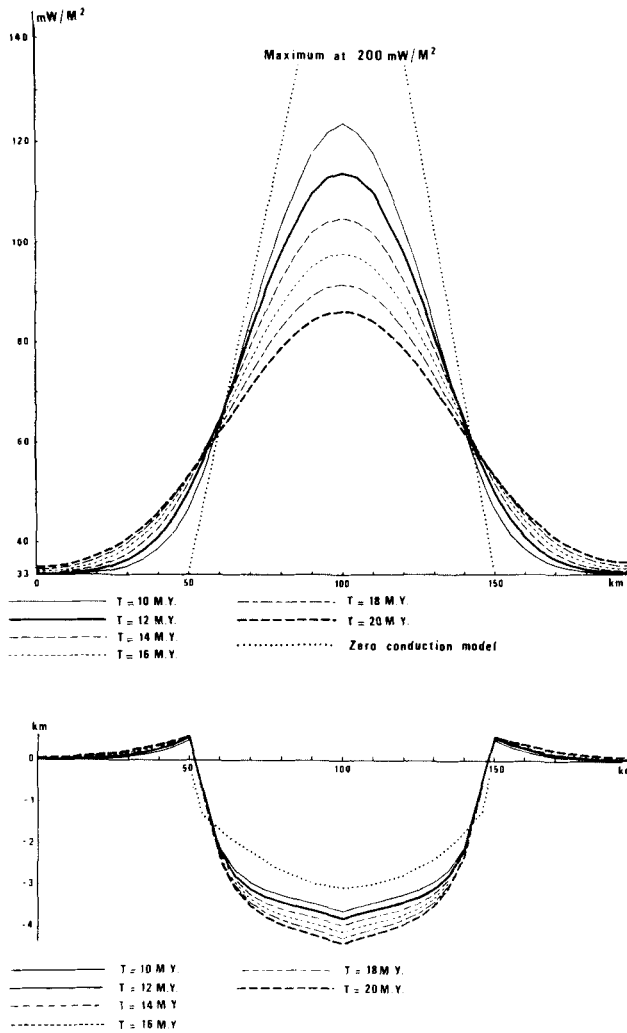


Figure 6. Thermal flux and subsidence are presented during the cooling phase from 10 to 20 Myr, every 2 Myr. The basin is the same as for Fig. 5.

effect $S_V = S_2 - S_1$ and the subsidence lateral conduction effect $S_L = S_3 - S_2$. Then, Fig. 7 shows that for the narrow basin, at the axis

$$\phi_3 = 0.52 \phi_1$$

whereas $\phi_2 = 0.90 \phi_1$,

thus $E_L = 3.8 E_V$. In the wide basin case (Fig. 9) $\phi_3 = 0.75 \phi_1$, thus $E_L = 1.5 E_V$.

In the same way, we see that $S_L = 1.75 S_V$ in the narrow basin case but $S_L = 0.25 S_V$ in the wide basin case.

In the following, we give empirical curves and relations to evaluate the necessity of using bidimensional computations rather than unidimensional ones during the stretching phases of continental margins. These estimations are valid for final extension factors at the axis β ranging from 2 to 6, total stretching times t from 10 to 30 Myr and half-widths of basin L (which is the width of one continental margin after stretching) ranging from 50 to

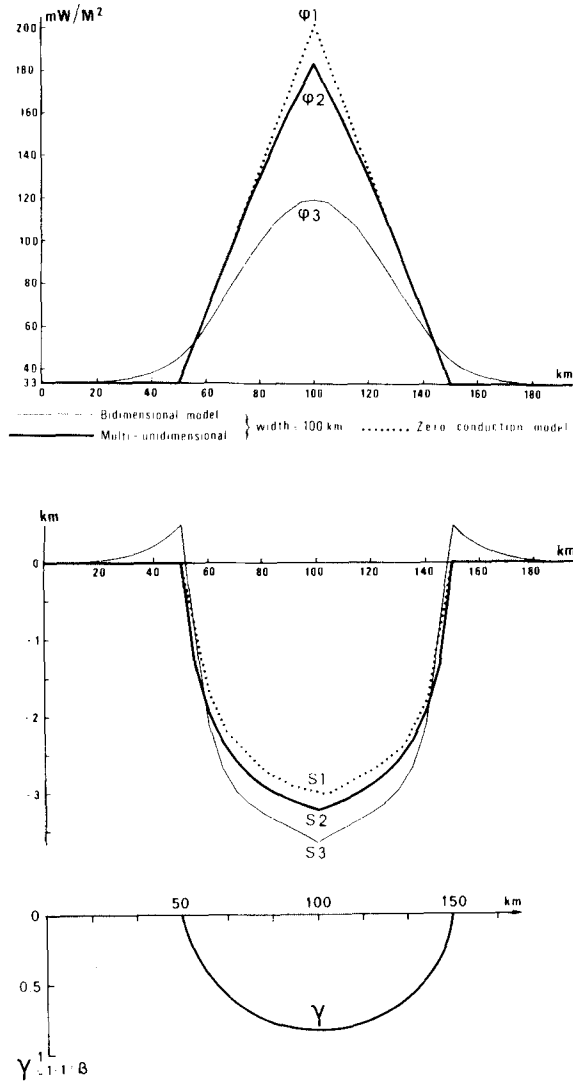


Figure 7. Three solutions are compared for the same hypothetical basin as for Fig. 5. The instantaneous stretching solutions are indexed by 1, the unidimensional by 2 and the bidimensional by 3. The thinning factor is displayed at the bottom of the figure.

200 km. As mentioned earlier, this set of parameters can be used to describe most continental margins.

Jarvis & McKenzie (1980) have shown that conduction can be ignored in the 1-D case if $t \cdot \beta^2 < 60 \text{ Myr}$ as the effect of β is to decrease the time constant of the lithosphere by $1/\beta^2$. In this case, E_L and E_V are small. We evaluate the relative effect of lateral and vertical conduction by computing the ratios E_L/E_V and S_L/S_V for variable axial β , t and L .

Fig. 11(a) shows the variation of E_L/E_V as a function of β for 10, 20 and 30 Myr total times. This ratio varies linearly with the ratio of the thickness of lithosphere h_L over the half-width of the basin L . In general, the lateral conduction effect is larger than the vertical one if L is of the order of h_L or smaller. The ratio is maximum for a value of β close to 2.

It goes toward 0 when β tends towards infinity. It is larger than 0.2 over most margins and basins of high stretching ratios ($\beta > 2$). Actually a good empirical fit can be obtained by

$$E_L/E_V = K(t) \beta^{-1.6} h_L/L; \quad \beta \geq 2. \tag{14}$$

$K(t)$ varies approximately as $175/t$ for t larger than 15 Myr and smaller than 50 Myr.

Fig. 11(b) shows the variation of S_L/S_V as a function of t for $L = 50, 125$ and 200 km. This variation is independent of β ; in other words, S_L and S_V have the same dependence on β . A good empirical fit can be obtained by

$$S_L/S_V = 14.4 \exp(-2L/h_L) t^{-1/2}. \tag{15}$$

The lateral conduction effect is smaller than the vertical one if L is larger than about 75–100 km. The lateral effect becomes negligible ($S_L/S_V < 0.2$) for L larger than about 200 km. Note that relations (14) and (15) have no meaning if E_V and S_V are small and

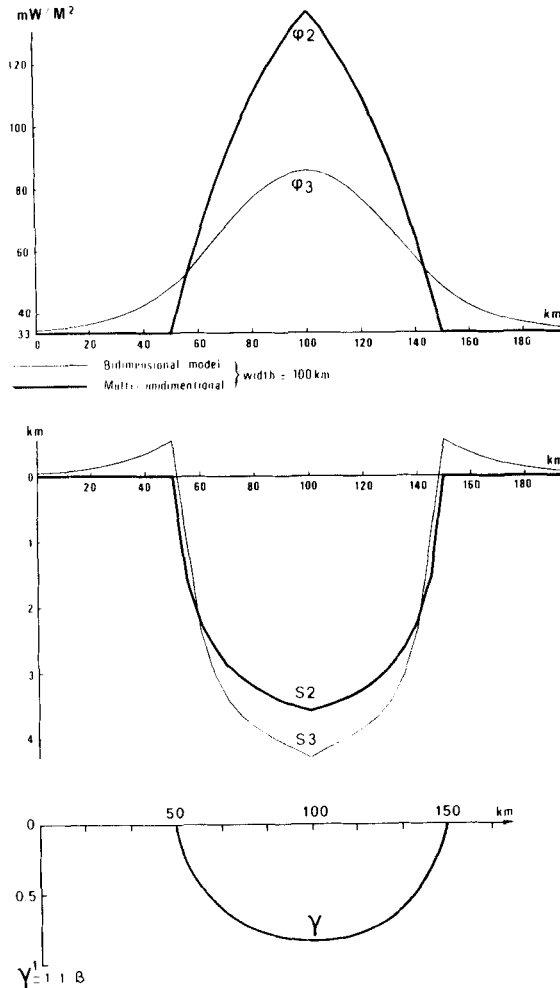


Figure 8. Three solutions are compared for the same hypothetical basin as for Fig. 6, except that the extension duration is now 30 Myr instead of 10 Myr as in Fig. 7.

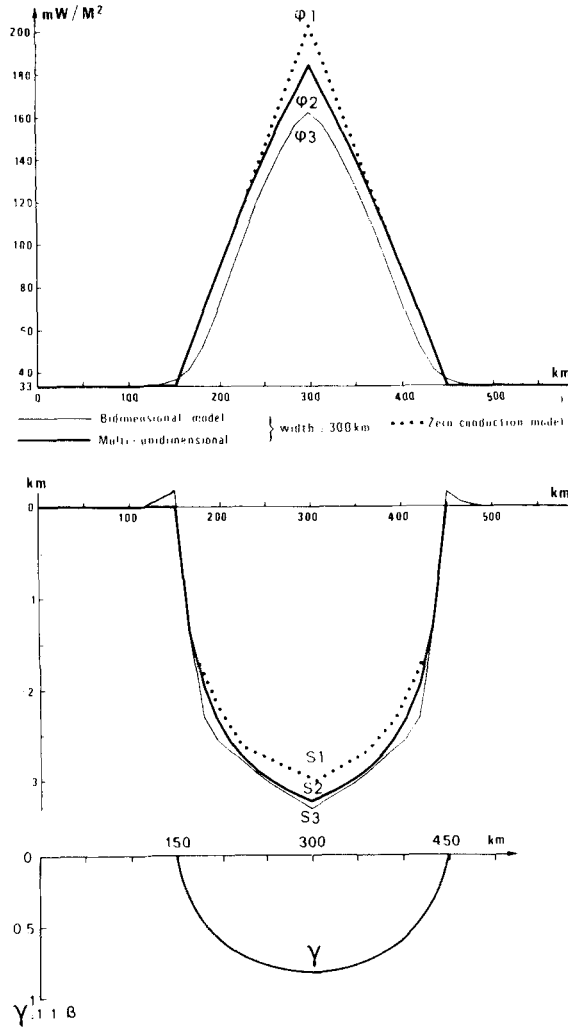


Figure 9. The final width of the basin is 300 km instead of 100 km and the extension duration is 10 Myr.

consequently if $t < 60/\beta^2$. Thus, they will in general be meaningless for $\beta < 2$. On the other hand, both relations can be used with a good approximation to evaluate the effect of increasing L .

Consider continental margins where L may go from 50 to 200 km and maximum β is of the order of 3–6; the above results indicate that the horizontal conduction effect dominates the vertical one over most margins and in general cannot be ignored. Note that, in percentage, much larger errors occur on the flanks of the basins if one ignores lateral conduction. Actually, the errors in computation of excess heat flow and elevation are infinite on the edges of the basins! We conclude that, over continental margins, 1-D computations do not represent a significant improvement over the instantaneous (zero conduction) approximation. If there is a significant conduction effect, then bidimensional computations are necessary.

Finally, we have computed the variation of the thermal uplift on the edges of a symmetrical basin as a function of total time t , axial β and half-width L . Fig. 11(c) shows

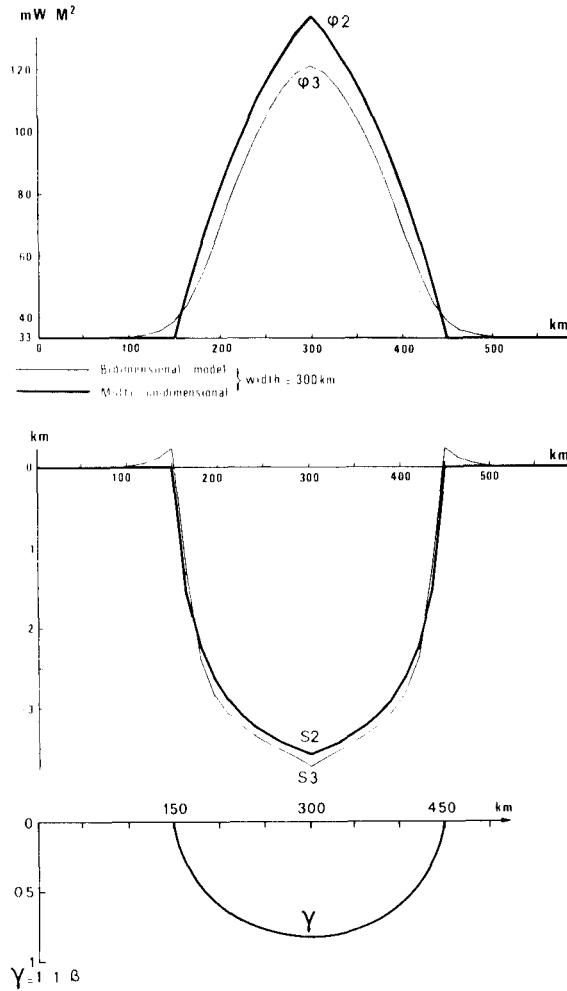


Figure 10. The final width of the basin is 300 km and the extension duration is 30 Myr.

this uplift as a function of time and stretching factor. A good empirical fit is obtained for the height B of the uplift by using:

$$B = 21.5 t^{0.213} \beta h_L / L \quad 5 < t < 50 \tag{16}$$

where B is in metres and t in Myr.

Equation (16) indicates that B , as the heat flow, varies linearly with the ratio h_L/L . It is consequently possible to predict the amplitude of B with a good approximation. In most geologically plausible cases, the thermal uplift will not exceed a value of 500 m. It will in general be two to three times smaller and the maximum value will be obtained with t of the order of 30 Myr.

Temperature profiles and partial melting

Figs 12–15 show the temperature sections corresponding to Figs 7–10. Note that the horizontal scale is normalized to the width of the basin (vertical exaggeration is $2.5 L/h_L$,

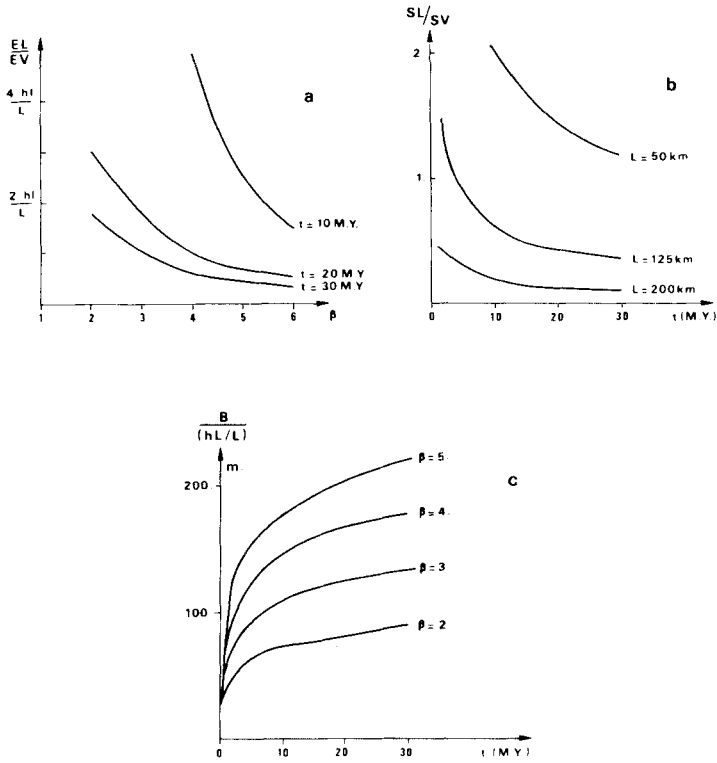


Figure 11. (a) Variation of E_L/E_V with respect to extension factor β for extension duration of 10, 20 and 30 Myr. (b) Variation of S_L/S_V with respect to time for different basins, where L is the half-width of the basin. (c) Variation of a scaled lateral uplift with respect to time for different extension factors β . The scaling factor is h_L/L , which is the thickness of the lithosphere over the width of the lithosphere.

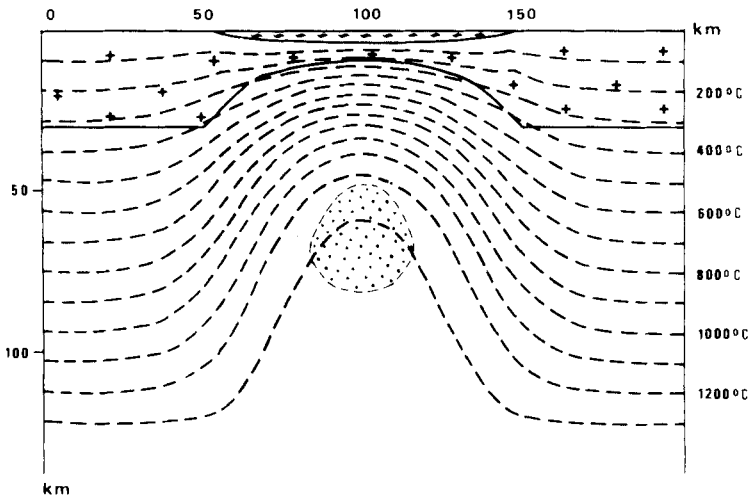


Figure 12. Isothermal contours for the hypothetical basin of Fig. 5, at the end of the extension. Partial melting zone is the shaded area.

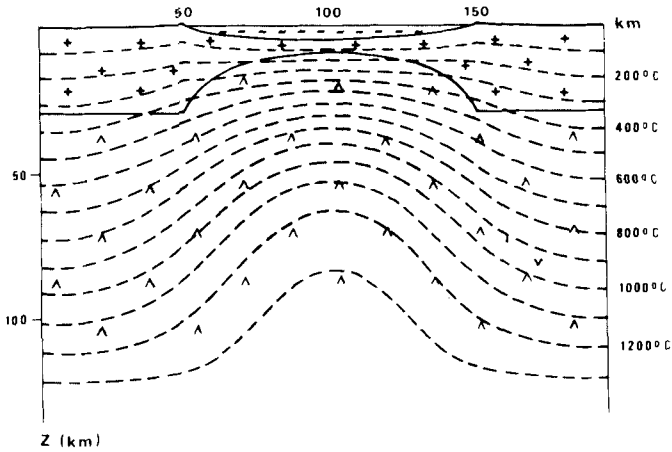


Figure 13. Isothermal contours for the hypothetical basin of Fig. 8, at the end of extension.

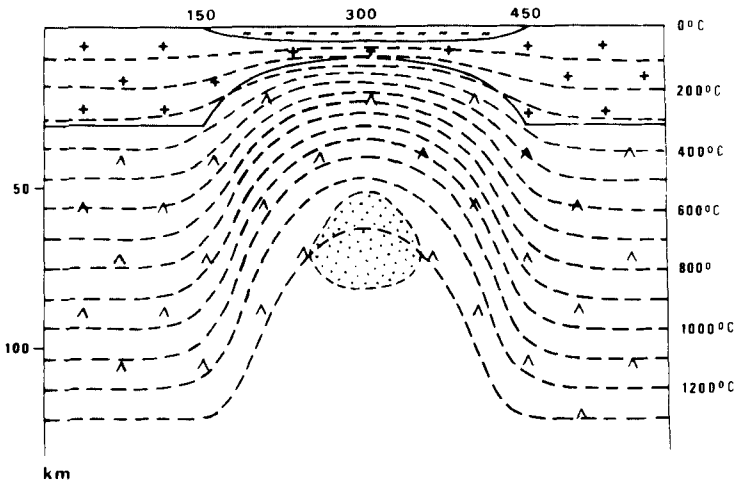


Figure 14. Isothermal contours for the hypothetical basin of Fig. 9, at the end of extension.

which is 1 for $L = 50$ km and 3 for $L = 150$ km). Thus, in the absence of conduction, Figs 12–15 should be identical, and the 320°C isotherm should coincide with the base of the continental crust. Obviously this is not the case and the difference is much larger for $L = 50$ km (Figs 12 and 13) than for $L = 150$ km (Figs 14 and 15).

Following Le Pichon *et al.* (1984) we ask what is the value of L below which the cooling will be sufficiently large to prevent the possibility of melting and thus prevent the formation of oceanic crust. Our investigation here is only qualitative and we use the very simple melting relationship proposed by Foucher, Le Pichon & Sibuet (1982) $T_m = 1100 + 3Z$, where Z is in km and T_m is in $^\circ\text{C}$. Then it is seen in Fig. 12 that there will be very limited melting for $L = 50$ km whereas large-scale melting exists for $L = 150$ km (Fig. 14). Actually, with the melting relationship adopted here, oceanic crust formation requires $L > h_L \sqrt{1.6/t}$, where t is the total stretching time in Myr. For reasonable stretching times (10–20 Myr), a minimum width of the stretched basin is $2L \sim 70$ – 100 km which is equivalent to 40–60 km for the unstretched width (using a linear distribution of γ ,

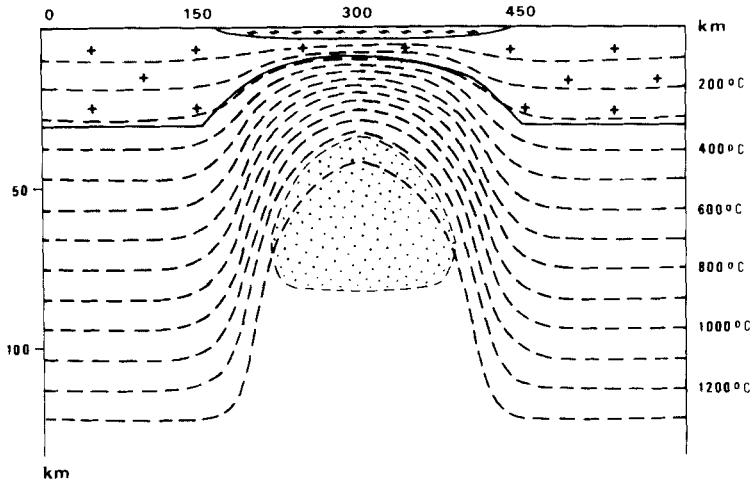


Figure 15. Isothermal contours for the hypothetical basin of Fig. 10, at the end of extension.

Le Pichon & Sibuet 1981). Thus Le Pichon *et al.* (1984) have argued that it is unlikely that the North Aegean trough will ever reach the oceanization stage in spite of high stretching factors. We conclude that lateral conduction imposes a minimum width to a continental margin and that this width may be of the order of 35–50 km if the melting relationship used here is approximately correct.

Bidimensional computations with sedimentation

De Bremaecker (1984) has shown that sedimentation need to be taken into account in thermal computations if the sedimentation rate is larger than 100 m Myr^{-1} . To illustrate the effect of sedimentation, we consider the same cases as previously (narrow $L = 50 \text{ km}$ and wide $L = 150 \text{ km}$ stretched continental margins) with a total sediment thickness of 1 and 5 km deposited during the 10 Myr long stretching phase at the axis of the trough. The variation of sediment thickness with time is linear. The lateral variation of sediment thickness is chosen to be proportional to γ (which is the proportion of crust removed by stretching). The distributions of heat flow and subsidence at the end of the 10 Myr long stretching phase are shown in Figs 16 and 17. Note that, as mentioned earlier, 5 km in 10 Myr is a very high rate of sedimentation for a basin produced by extension. For example, synrift sediment thickness is only about 2 km on the Western Mediterranean margins (Le Douaran *et al.* 1984) and much less on the Armorican margin (Montadert *et al.* 1979). In the Gulf of Suez, 2.5 km of synrift sediments were accumulated in 20 Myr since Lower Miocene (Garfunkel & Bartov 1977). Only in the North Aegean trough do we find a rate of sedimentation equivalent to 500 m Myr^{-1} (5 km in 10 Myr, Le Pichon *et al.* 1984).

In the computations, we take into account the effect of compaction on sediments. This is done by adopting exponential variations of density, conductivity and heat capacity with depth. It is well known that, to the first order, density within sediment ρ_s varies linearly with porosity. In the same way, the thermal conductivity K_s varies approximately linearly with porosity (Sclater & Christie 1980). Finally, the volumetric heat capacity $\rho_s c_s$ is the sum of the heat capacity of the solid and liquid phases and consequently also varies approximately linearly with depth. As the porosity closely follow, an exponential variation with depth

(Sclater & Christie 1980), the variation with depth of the three parameters ρ_s , K_s and $\rho_s c_s$ can be approximated by the same exponential decrease.

To determine this rate of exponential decrease, we use the study of the North Aegean trough by Le Pichon *et al.* (1984) because 5 km of sediments accumulated there in only 10 Myr. The density law of variation with depth, which was obtained indirectly through compressional velocity determinations, determines the rate of exponential decrease with depth. At the seafloor (for $Z = 0$), the values adopted are in agreement with those measured by Jongma (1974) in the North Aegean trough. For large Z , the adopted values are reasonable for the upper crust. The three relations are given in Table 1.

Note that the conductivity approximately doubles from the surface to a depth of 5 km

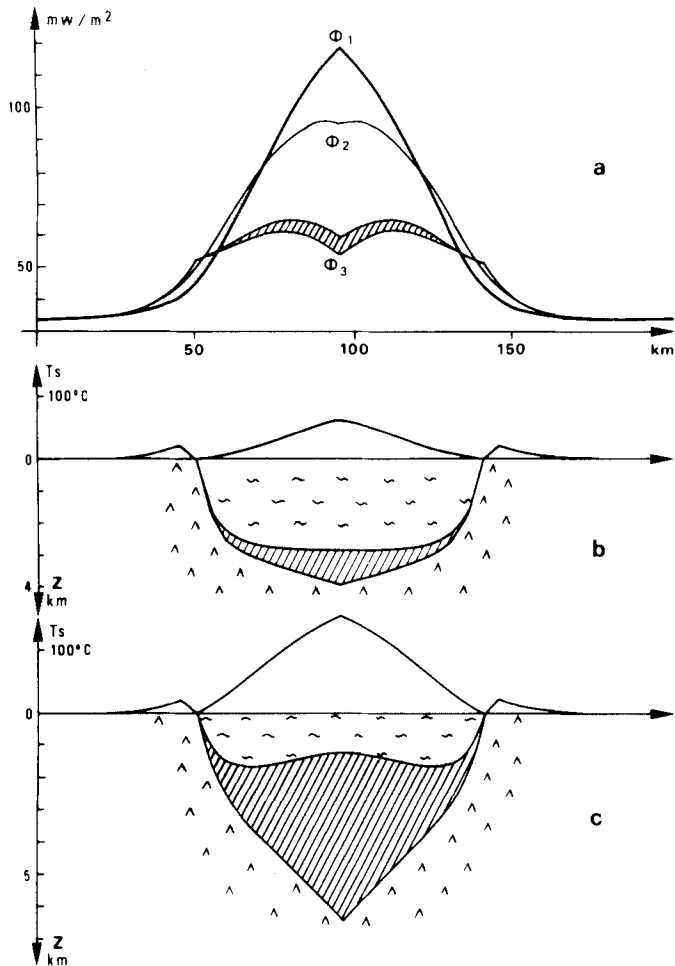


Figure 16. Thermal computations across an hypothetical sedimentary basin with a final width of 100 km. The extension factor distribution is symmetrical, with a maximum extension factor of 6 at the axis after 10 Myr. The total sediment thickness deposited during the 10 Myr are 1 km (case 1) and 5 km (case 2). Thermal flux, subsidence and temperatures at the bottom of the sedimentary layer are presented. (a) ϕ_1 : thermal flux over the basin without sediment. ϕ_2 : thermal flux over the sedimentary basin (case 1) (dashed area represent the portion of the flux absorbed by the sediment). ϕ_3 : thermal flux over the sedimentary basin (case 2). (b) Above the horizontal axis, temperature at the bottom of the sedimentary layer, below the computed topography and basement for case 1 (dashed lines represent sedimentary layer). (c) Same as (b) for case 2.

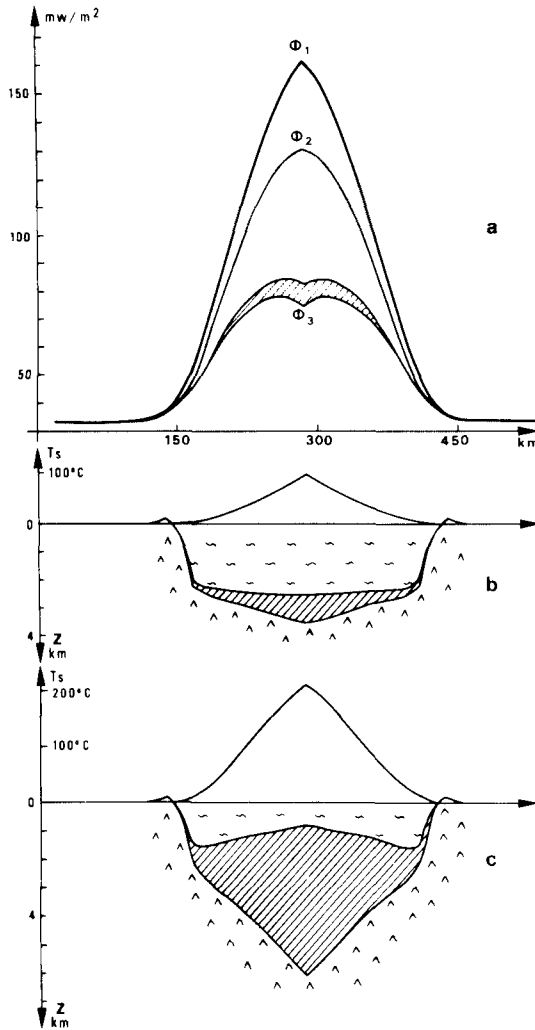


Figure 17. Thermal computations across an hypothetical sedimentary basin with a final width of 300 km. The extension factor distribution is symmetrical, with a maximum extension factor of 6 at the axis after 10 Myr. The total sediment thickness deposited during the 10 Myr are 1 km (case 1) and 5 km (case 2). Thermal flux, subsidence and temperatures at the bottom of the sedimentary layer are presented. (a), (b) and (c) as in Fig. 16.

where it is close to the conductivity of the crust. But the volumetric heat capacity is halved over the same interval because of the much larger heat capacity of water. Thus, the diffusivity increases by a factor of 4 from the surface to 5 km depth. However the exponential variation is such that at a depth of 2 km, 80 per cent of the variation has already occurred and any further change with depth is small. This is why the equivalent diffusivity for a 5 km thick sedimentary basin is close to the value for the asthenosphere.

Knowing the law of variation of thermal conductivity and volumetric heat capacity with depth within the sediments, our method requires the determination of a single equivalent conductivity and heat capacity for the whole layer. For the heat capacity, we simply take the arithmetic mean $\rho_s c_s$. However, for the conductivity, we need to take the harmonic

mean \bar{K} , where

$$\frac{1}{\bar{K}} = \frac{1}{Z_h} \int_0^{Z_h} dZ/K(Z).$$

This is done at each time step for the corresponding sediment layer.

Figs 16 and 17 show that the heat flow at the axis is greatly reduced by the sedimentation. This reduction is about 20 and 65 per cent respectively for the 1 and 5 km thicknesses. However, there is a significant lateral conduction effect and the reduction depends on the width of the basin. It is 22 per cent in the narrow basin ($L = 50$ km), instead of 19 per cent in the wide basin ($L = 150$ km) for the 1 km case and 68 instead of 60 per cent for the 5 km case.

On the other hand, the tectonic subsidence (subsidence obtained by removal of the sediment layer and local isostatic readjustment) does not change significantly with the presence of sediment. The introduction of the sedimentary layer does not modify sufficiently the thermal structure of the lithosphere at depth, in such a small amount of time (10 Myr) to produce variations in tectonic subsidence. The changes correspond to 20 and 60 m of increase of tectonic subsidence for $L = 50$ km and 20 and 70 m for $L = 150$ km. Thus, the modification of the subsidence is only due to the weight of the sedimentary layer and the consequent isostatic readjustment. We conclude that to obtain the subsidence during the early margin rifting phase, one does not need to include the effect of sedimentation in the thermal computations whereas this is absolutely necessary when computing the heat flow.

Finally, we show in Figs 16 and 17 the predicted temperatures at the bases of the sedimentary sections. For $L = 50$ km, the maximum temperatures reached are 70°C for 1 km thickness and 175°C for 5 km thickness whereas for $L = 150$ km they are 90 and 245°C. The effect of compaction is the principal cause of the non-linear increase of temperature with sedimentary thickness. Using a formula such as the one given by Royden *et al.* (1980), it would be simple to obtain the corresponding maturation index for each case.

Conclusion

We have presented a numerical method to compute the thermal evolution of a lithosphere submitted to laterally variable stretching. The method incorporates the effect of sedimentation by considering the sedimentary cover as perturbing the surface temperature condition. The initial horizontal strain rate distribution is obtained from the final distribution of stretching factors with the hypothesis that strain rate for a given column of particles is independent of depth and time. The accuracy of the method has been tested by comparing it to unidimensional analytical solutions. It is excellent in the absence of sedimentation but the accuracy deteriorates when sedimentation rates equal to or larger than about 500 m My⁻¹ are adopted.

The main conclusion of our work is that lateral conduction introduces significant changes in the evolution of the rifting phase of a continental margin. In particular, the lateral conduction effect is larger than the vertical one over most continental margins during their stretching. We propose a way to evaluate the relative importance of lateral and vertical conduction effects at the axis of a zone of rifting just prior to oceanization. We show that, if the initial width of the zone of stretching is less than 40–60 km, lateral conduction will be so strong as to prevent the possibility of melting and consequently prevent the oceanization for reasonable stretching times ($t \geq 10$ Myr). Thus, an unsedimented continental margin should have a minimum width of 35–50 km.

We propose a simple way to evaluate the amplitude of the thermal uplift on the edges of the zone of rifting. The thermal uplift does not exceed 500 m for reasonable geological conditions. It is in general two to three times smaller.

Finally, we discuss the effects of high sedimentation rates. The effect of the sedimentation is to increase the surface temperature of the lithosphere and consequently to significantly decrease the surface heat flow. However, the tectonic subsidence is not significantly changed by high sedimentation rates during a time of the order of 10 Myr.

Acknowledgments

The idea on which this work started came from the thesis of P. Watremez, A. Benezra and D. Lefebvre developed a first version of the computer program. The work was financially supported by Total and Elf. Support from CNRS and CNEXO is also acknowledged. We acknowledge the comments of an anonymous referee who pointed out in particular that we should use the harmonic mean to obtain the equivalent conductivity within the sedimentary layer.

References

- Angelier, J. & Colletta, B., 1983. Tension fractures and extensional tectonics, *Nature*, **301**, 49–51.
- Beaumont, C., Keen, C. E. & Boutillier, R., 1982. On the evolution of rifted continental margins: comparison of models and observations for the Nova Scotian margin, *Geophys. J. R. astr. Soc.*, **70**, 667–715.
- Carslaw, H. S. & Jaeger, J. C., 1959. *Conduction of Heat in Solids*, Clarendon Press, Oxford.
- De Bremaecker, J. C., 1984. Temperature, subsidence and hydrocarbon maturation in extensional basins: a finite element model, *Am. Ass. Petrol. Geol.*, in press.
- Douglas, J., 1955. On the numerical integration of $\partial^2 u / \partial x^2 + \partial^2 u / \partial y^2 = \partial u / \partial t$ by implicit methods, *J. Soc. indust. appl. Math.*, **3**, 42–65.
- Foucher, J. P., Le Pichon, X. & Sibuet, J. C., 1982. The ocean-continent transition in the uniform lithospheric stretching model: role of partial melting in the mantle, *Phil. Trans. R. Soc. A*, **305**, 27–43.
- Garfunkel, Z. & Bartov, Y., 1977. The tectonics of the Suez Rift, *Bull. geol. Surv. Israël*, **71**, 1–44.
- Jarvis, G. T. & McKenzie, D. P., 1980. Sedimentary basin formation with finite extension rates, *Earth planet. Sci. Lett.*, **48**, 42–52.
- Jongsma, D., 1974. Heat flow in the Aegean Sea, *Geophys. J. R. astr. Soc.*, **37**, 337–346.
- Le Douaran, S., Burrus, J. & Avedik, F., 1984. Deep structure of the North Western Mediterranean basin: results of a two ships seismic survey, *Tectonophysics*, in press.
- Le Pichon, X. & Sibuet, J. C., 1981. Passive margins: a model of formation, *J. geophys. Res.*, **86**, 3708–3720.
- Le Pichon, X., Angelier, J. & Sibuet, J. C., 1982. Plate boundary and extensional tectonics, *Tectonophysics*, **81**, 239–256.
- Le Pichon, X., Lyberis, N. & Alvarez, F., 1984. The North Aegean trough. Part 2. Subsidence, *J. geol. Soc. London*, in press.
- Marchuk, G. I., 1975. *Methods of Numerical Mathematics*, Springer-Verlag, New York.
- McKenzie, D. P., 1978. Some remarks on the development of sedimentary basins, *Earth planet. Sci. Lett.*, **40**, 25–32.
- Montadert, L., Roberts, D. G., de Charpal, O. & Guennoc, P., 1979. Rifting and subsidence of the Northern continental margin of the Bay of Biscay, *Init. Rep. Deep Sea drill. Proj.*, **48**, 1025–1060.
- Peaceman, D. W. & Racheford, H. H., 1955. The numerical solution of parabolic and elliptic differential equation, *J. Soc. indust. appl. Math.*, **3**, 20–41.
- Royden, L., Sclater, J. G. & Von Herzen, R. P., 1980. Continental margin subsidence and heat flow, important parameters in formation of petroleum hydrocarbon, *Bull. Am. Ass. Petrol. Geol.*, **64**, 173–187.
- Royden, L. & Keen, C. E., 1980. Rifting process and thermal evolution of the continental margin of Eastern Canada determined from subsidence curves, *Earth planet. Sci. Lett.*, **51**, 343–361.
- Sclater, J. G. & Christie, P. A. F., 1980. Continental stretching: an explanation of the post-mid-Cretaceous subsidence of the Central North sea basin, *J. geophys. Res.*, **85**, 3711–3739.

Appendix A: numerical scheme of thermal problem

The numerical method we are using is a straightforward extension of the splitting-up method developed by Peaceman & Rachford (1955) and Douglas (1955), by including convective terms.

At a given point in space ($i\Delta x, j\Delta z$) and in time $(2n+1)\Delta t$, the temperature is noted $T_{i,j}^{2n+1}$. Δx is the horizontal grid step, Δz is the vertical one, and Δt is the time step.

By using splitting-up technic, temperature distribution at time $(2n+2)\Delta t$ is deduced from temperature distribution at time $2n\Delta t$, with the following two-step procedure.

$$\begin{aligned} \frac{T_{ij}^{2n+1} - T_{i,j}^{2n}}{\Delta t} &= \frac{k}{\rho C_p} \left(\frac{T_{i-1,j}^{2n+1} + T_{i+1,j}^{2n+1} - 2T_{i,j}^{2n+1}}{\Delta x^2} + \frac{T_{i,j-1}^{2n} + T_{i,j+1}^{2n} - 2T_{i,j}^{2n}}{\Delta y^2} \right) \\ &\quad - v_{i,j}^{2n+1/2} \frac{T_{i+1,j}^{2n+1} - T_{i-1,j}^{2n+1}}{2\Delta x} - u_{i,j}^{2n+1/2} \frac{T_{i,j+1}^{2n} - T_{i,j-1}^{2n}}{2\Delta y} + C_{i,j}^{2n+1/2} \\ \frac{T_{i,j}^{2n+2} - T_{i,j}^{2n+1}}{t} &= \frac{k}{\rho C_p} \left(\frac{T_{i-1,j}^{2n+1} + T_{i+1,j}^{2n+1} - 2T_{i,j}^{2n+1}}{\Delta x^2} + \frac{T_{i,j-1}^{2n+2} + T_{i,j+1}^{2n+2} - 2T_{i,j}^{2n+2}}{\Delta y^2} \right) \\ &\quad - v_{i,j}^{2n+3/2} \frac{T_{i+1,j}^{2n+1} - T_{i-1,j}^{2n+1}}{2\Delta x} - u_{i,j}^{2n+3/2} \frac{T_{i,j+1}^{2n+2} - T_{i,j-1}^{2n+2}}{2\Delta y} + C_{i,j}^{2n+3/2}. \end{aligned}$$

The velocity distribution is assumed to be known at any point in space ($i\Delta x, j\Delta z$) and in time $(2n+1/2)\Delta t$. Velocity is noted $(v_{i,j}^{2n+1/2}, u_{i,j}^{2n+1/2})$ where v is the horizontal component and u the vertical one. The internal heat production is given by $C_{i,j}^{2n+1/2}$ at the same point.

Appendix B: instantaneous extension coefficient evaluation

The differential equation (5) has to be solved numerically in the moving frame (Lagrange's frame). The present instantaneous extension coefficient distribution will be the 'initial' condition of the resolution by going backwards in time (noted by $e = -1$). By this way, the instantaneous extension coefficient distribution, at the initiation of the extension, is obtained. This distribution will be the initial condition when solving equation (5) by going forwards in time (noted by $e = 1$), during thermal computations.

At every time needed by thermal computation, instantaneous extension coefficients are evaluated in the fixed frame (Euler's frame) from the moving frame, by interpolation.

The numerical discretization of equation (5) is obtained by Euler's method:

$$\frac{l_i^{t+e\Delta t} - l_i^t}{e\Delta t l_i^t} = \frac{1}{2} (g_{i+e}^t + g_i^t)$$

where l_i^t is the position of the i th point at time t in the moving frame, with respect to the fixed point where extension is initiated.

Appendix C: sedimentary layer: its thermal equilibrium

The thermal perturbation of sediments is taking into account by modifying the temperature condition at the top of lithosphere. Assuming that sediments are in thermal equilibrium at each time $n\Delta t$, and knowing the thermal flux at the top of the lithosphere ϕ_b^n , allow to

evaluate the mean temperature T_m^n inside sediments by

$$T_m^n = h_s^n \phi_b^n / 2 \bar{k}_s^n$$

where h_s^n is the sedimentary thickness and \bar{k}_s^n is the mean harmonic sedimentary conductivity. Vertical heat transfer is also assumed inside elements.

Because sediments are in thermal equilibrium (constant temperature gradient), the temperature at the lithosphere-sediment boundary is given by

$$T_b^n = 2 T_m^n.$$

This temperature will be the new temperature condition at the top of the lithosphere for the next time step.

A more accurate surface heat flux can be made by taking into account heat dQ_1^n absorbed by sediments to increase its mean temperature from T_m^{n-1} to T_m^n :

$$dQ_1^n = \{ T_m^n h_s^n - T_m^{n-1} h_s^{n-1} \} (\overline{\rho_s C_p})^n + T_m^n (\overline{\rho_s C_p})^n g_i \Delta t.$$

The last term comes from sedimentary layer extension. Therefore the surface heat flux is deduced:

$$\phi_s^n = \phi_b^n - dQ_1^n / \Delta t$$

lower than the bottom heat flux.

Mean values, inside sediments, are obtained by using the following depth-dependent laws:

$$\rho_s(z) = \rho_0 - \rho_\lambda \exp(-Z/\lambda)$$

$$K_s(z) = K_0 - K_\lambda \exp(-Z/\lambda) \tag{see Table 1}$$

$$(\rho_s C_p)(z) = (\rho_s C_p)_0 - (\rho_s C_p)_\lambda \exp(-Z/\lambda).$$